This article has been accepted for publication in a future proceedings of this conference, but has not been fully edited. Content may change prior to final publication. Citation information: DOI10.1109/UPEC57427.2023.10295005, 2023 58th International Universities Power Engineering Conference (UPEC)

Potential Benefits and Challenges of Employing Inertia Distribution Indexing in RMS Simulations

Stephen Sommerville
Department of Electronic & Electrical Engineering
Brunel University London, Uxbridge, UK
stephen.sommerville@brunel.ac.uk

Professor Gareth A Taylor
Department of Electronic & Electrical Engineering
Brunel University London, Uxbridge, UK
gareth.taylor@brunel.ac.uk

Professor Maysam Abbod
Department of Electronic & Electrical Engineering
Brunel University London, Uxbridge, UK
maysam.abbod@brunel.ac.uk

***Abstract*—Globally there has been a trend towards increasing penetration of Converter Fed Generation (CFG) into main power systems, and a reduction of conventional synchronous generation. One of the recent research areas, that has attracted some significant consideration is the uneven distribution of inertia through a power system and the potential local variations of frequency and Rate of Change of Frequency (RoCoF). This paper uses the IEEE 9-Bus test network to develop show how measurement of frequency within RMS simulation packages is of critical importance and that the current use of an Inertia Distribution Index (IDI) can overlook critical generators when a very uneven distribution of inertia exists. An alternative, based on frequency difference magnitude, is developed in this paper as a more robust approach.**

Keywords—frequency stability, inertia, inertia distribution, PowerFactory, RoCoF.

I. Introduction

A. Introduction

This paper focuses on power system stability, and specifically on frequency stability and how uneven distribution of inertia within a power system can lead to localized variations in frequency and Rate of Change of Frequency (RoCoF) and impact the of Converter Fed Generation (CFG) on system performance. The report shows the derivation of the concept of Centre of Inertia (COI) from first principles using the Swing Equation, and subsequently uses the concept of COI with an Inertia Distribution Indexation (IDI) approach to classify local frequency variations. Finally, the report shows some outline analysis of the concepts using the IEEE-9 Bus test network, using DIgSILENT PowerFactory.

B. Background

The concept of power system stability has been a well-studied area, with numerous textbooks on the subject. Power system stability problems have classically been split into three main areas known as frequency stability, voltage stability and rotor angle stability, which are then further sub-divided into different areas for analysis [1]. Recent developments in renewable technologies have led to wider definition of stability classifications to include systems with high penetration of renewable technologies which expand the original three definitions to also include resonance stability and convertor stability [2].

A recent development in modern power systems with a high penetration of CFG, is that the decreasing levels of inertia can have a significant effect on the system RoCoF during a frequency disturbance [3]. A number of studies and papers have sought to explore this issue further by considering solutions based on Synchronous Condensers to support existing Grid Following Inverters (GFL), before the future generation of Grid Forming Inverters (GFI) reaches large scale deployment [4]–[8].

The increased level of CFG dominated systems, and the use of Synchronous Condensers has created an interest in how decreasing system inertia, can also be impacted by the locational specific distribution of inertia, as this can give significant localized variations in RoCoF in areas that are remote from the system Centre of Inertia (COI). The general concept of COI has been utilized for a large number of years and can be seen in a number of key papers [9]–[15].

The potential significance of considering localized inertia variations, allows weak spots in the network to be identified and possible locations for Fast Frequency Response (FFR) services or synchronous condensers to be added to the network to help stabilize the system RoCoF during outage cases.

C. Contributions to Knowledge

The contribution to knowledge in this paper is to analyse the importance of inertia distribution in the IEEE 9-Bus test network and show how very uneven inertia distributions within a system can produce significant variations in network response. The paper indicates how the use of frequency measurement within RMS simulations packages can significantly impact the results. Lastly the paper shows that the currently proposed use of an IDI approach can overlook the importance of generators in certain scenarios and proposes a simpler calculation method for determine the system vulnerability.

D. Frequency Stability and RoCoF

One of the key concepts within frequency stability analysis is the equations of motion that describe the unbalance between the mechanical torque and electromechanical torque of synchronous machines in the system. The Swing Equation is generally regarded as a good approximation of how the frequency responds to a change in change in power in the system, based on the system capacity and the available inertia. Various derivations are given for this, such as Kundur [1], with the equations shown in (1) and (2).

$$\frac{2H}{\omega_s}\frac{d^2\delta}{dt^2} = P_m - P_e = P_a \tag{1}$$

$$\frac{df}{dt} = \frac{P_{in} - P_{out}}{2SH} f = \frac{\Delta P}{2I} f \tag{2}$$

Inertia is of specific interest in frequency stability, as the inertia operates automatically and instantaneously, and limits the RoCoF, whilst the system primary frequency response

This article has been accepted for publication in a future proceedings of this conference, but has not been fully edited. Content may change prior to final publication. Citation information: DOI10.1109/UPEC57427.2023.10295005, 2023 58th International Universities Power Engineering Conference (UPEC)

(PFR) begins to operate. It is evident that the lower the system inertia the faster the RoCoF and greater the frequency nadir reached before the PFR systems can begin to operate. Thus, any localized variations of inertia and RoCoF are of key interest to system operators.

E. Loss of Mains (LoM) and RoCoF

Many countries within Europe, as well as Australia use RoCoF as one of the methods for detecting a Loss of Mains (LoM) failure, and a basis for tripping embedded generators to prevent islands from forming. Furthermore, excessive values of RoCoF can also lead to problems of operation of conventional thermal generators, such as gas and coal fired plants may not successfully ride through RoCoF values much > 1 Hz/s and some concerns have also been raised in relation to the satisfactory operation of underfrequency relays not operating satisfactorily of the RoCoF at > 2 Hz/s and can have significant problems at values of > 3 Hz/s. With the UK, National Grid ESO defines the RoCoF limit as 1 Hz/s over a 500 ms sample window [16]; ENTSO-E guidelines are that the RoCoF should be limited to 1Hz/s over a 500 ms window [17], [18]; AEMO guidelines are also that the RoCoF should be limited to 1 Hz/s over a 500 ms window [19].

II. Centre of Inertia and Inertia Distribution Indexing

A. Centre of Inertia

As noted in section I.D, the overall system inertia can be calculated through the summation of all the system inertia in the network. As with an equivalent mechanical system, the Centre of Inertia (COI) of the system is of interest, as this is the weighted average of the network, which is used for calculation purposes and where the system is balanced. The COI is defined in Kundur [1] as the summation of all the inertia constants H_T of n generators in the system as shown in equation (3) and with the motion of the COI determined by equations (4) and (5).

$$\boldsymbol{\delta_{COI}} = \frac{\mathbf{1}}{\boldsymbol{H_T}} \sum_{\boldsymbol{i=1}}^{\boldsymbol{n}} \boldsymbol{H_i \delta_i} \tag{3}$$

$$2H_T p(\Delta\omega_{COI}) P_{COI} = \sum_{i=1}^{n} (P'_{mi} - P_{ei}) \tag{4}$$

$$P(\delta_{COI}) = (\Delta\omega_{COI})\omega_0 \tag{5}$$

B. Inertia Distribution and Indexing

The distribution of inertia within the system is of key importance as it can impact local RoCoF rates significantly. This can lead to system disturbances causing an unexpected RoCoF trip in embedded generation systems that are nearby, further exacerbating problems of system recovery. The use of an Inertia Distribution Index (IDI) can allow localized weak spots to be identified, that may be subject to higher RoCoF variations during system disturbances.

The frequency at the COI can be given by equation (6), as developed in [15] where the total number of generators is given by *ng* and H_i and f_i is the inertia and frequency of generator *i* at a given time *t*.

Once the frequency of the COI is determined along with the frequency of generator at busbar *k*. where the frequency of the local generator is compared with the frequency of the COI, and calculated using an integral square function, as detailed in equation (7).

In the final step an index value of dk can be determined for the generator. The index value of d_k can then be used to give an overall IDI value, by comparing it against the maximum value of d_k on the system as shown in equation (8). This returns an index value, where a high value indicates a busbar that either has a low concentration of inertia or is electrically distant from the COI, or both.

$$\boldsymbol{f_{COI(t)}} = \frac{\sum_{\boldsymbol{i=1}}^{\boldsymbol{ng}} \boldsymbol{H_i f_i}}{\sum_{\boldsymbol{i=1}}^{\boldsymbol{N}} \boldsymbol{H_i}} \tag{6}$$

$$d_k = \int_{t_0}^{T+t_o} \left(f_k(\tau) - f_{COI}(\tau)\right)^2 d\tau \tag{7}$$

$$IDI_k = \frac{d_k}{max\ d_k} \tag{8}$$

III. Frequency Measurement

A. Frequency Calculation in RMS Simulation

Most modern large scale power system analysis is carried out with commercial programs using RMS based analysis techniques. The use of RMS based analysis is known to contain several potential shortfalls in the detail of analysis, and the use of EMT simulations has also become more popular as a result [20]. For the analysis in this paper, the well-known simulation software DigSILENT PowerFactory.

B. Simple Test Network

A simple test network was created, based on the network used in [15] consisting of two 50 MW, generators connected by a series of identical length lines and intermediate busbars, to represent differing locations within the power system. The frequency is then measured at key busbars, to determine the localized variations. The network diagram can be seen below in Fig. 1.

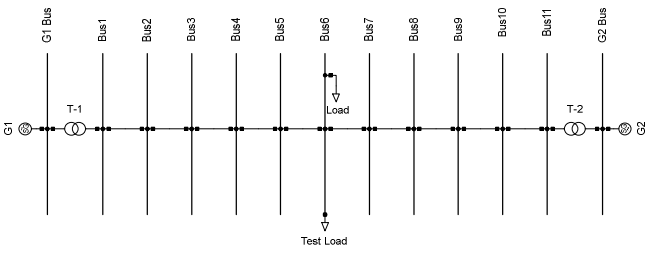

Fig. 1. Simple Test System

C. Frequency Measurement Techniques

When considering measurement of system frequency, it is possible to use several different techniques within the software package, but these can potentially give incorrect or misleading results. With the PowerFactory software, some

This article has been accepted for publication in a future proceedings of this conference, but has not been fully edited. Content may change prior to final publication. Citation information: DOI10.1109/UPEC57427.2023.10295005, 2023 58th International Universities Power Engineering Conference (UPEC)

different methods are possible, which will all give slightly different results. These are summarized below.

- A signal can be measured directly from a synchronous generator. This value is calculated directly by the mechanical equations of the machine and is considered to be very accurate.
- An 'indicative' frequency and frequency derivative signal can be calculated from individual busbars obtained from (*Phi(t)-Phi(t-dt))/dt*, where *dt* is the current time step and phi is the voltage angle at the busbar. There is no filtering of the value, which can result in sudden changes in values.
- Use of a voltage measurement device (StaVmeas), this is a simplified device which is used to mimic a typical frequency measurement device. It is also based on the voltage angle at the busbar and filtered over a span of 3 periods.
- Use of a PLL connected to the relevant busbars. The PLL is based on a standard SRF design with a PI controller and can be tuned and adjusted as required based on the system performance and required response.

D. Comparison of Results

The test network shown in Fig. 1, was analysed through application of a simple test load of 20 MW connected at the midpoint Busbar 6, at 0.2 s and then disconnected 500ms later, in order to identify the system frequency disturbance. Two different PLLs were used, both based on the standard DIgSILENT model; the untuned PLL was set with a default value of *Kp* (proportional gain) of 10 and *Ki* (integral gain) of 30; the other PLL was tuned to match the response of the G1 generator and resulted in a *Kp* of 1.5 and *Ki* of 100. The results of the simulation can be seen in Fig. 2, where it can be identified that there is a significant range in responses between the different techniques.

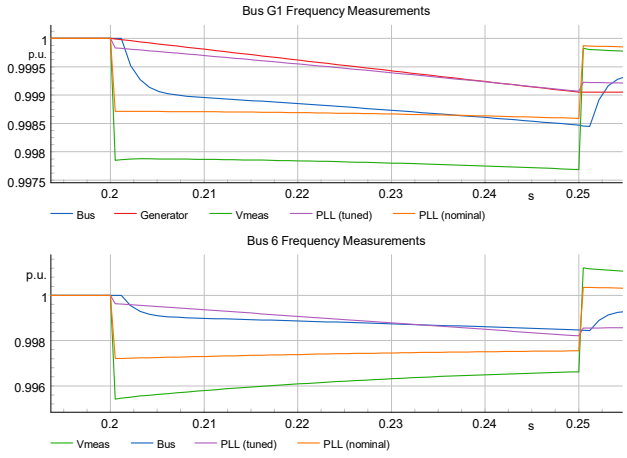

Fig. 2. Simple Test System Results

The response at G1 busbar indicates that the untuned PLL and device produce similar shaped responses, which are notably different to the more accurate results of the synchronous generator frequency. The tuned PLL most closely follows the generator frequency, and the direct busbar measurement response is like the untuned PLL, but with a smoother response. Similarly, the response at the Bus 6 busbar showed some significant differences between the frequency measurement devices but lacked the reference signal from a synchronous machine to compare against.

IV. IEEE 9-Bus Network

A. Base Configuration

For the analysis a typical test network was used based on the IEEE 9-Bus network. The configuration and distribution of the main generators and inertia is summarized in Table I, where it can be seen the total system inertia is 3472 MVA.s, with 68.1% located at G1, 21.7% located at G2 and 10.2% located at G3. A new 100 MW temporary load is connected Bus 8 and connected to the system at 0.2 s and disconnected 200 ms later. A voltage measurement device is added to the system as this allows the COI frequency to be extracted from the model. The IEEE 9-Bus model can be seen in Fig. 3.

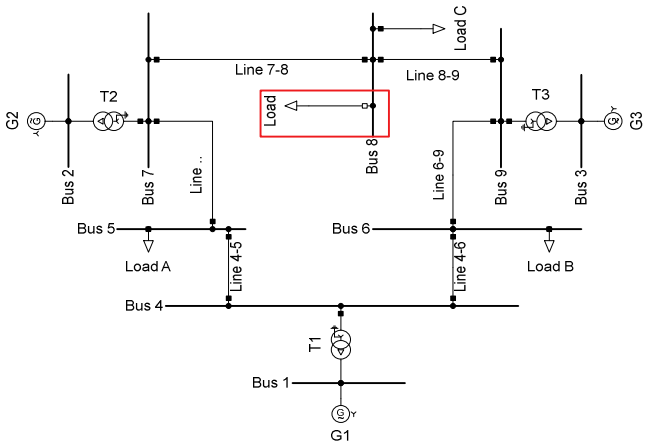

Fig. 3. IEEE 9-Bus Model

B. Weighted Inertia Distribution

To demonstrate the concepts and impacts of inertia distribution the IEEE 9-Bus network was modified slightly. The overall system inertia was calculated as 3470 MVA.s, and three network variations were created with increasing value of inertia located at the G1 machine, such that the G1 machine represented 80%, 90% and 95% of the overall system inertia. This can be seen in Table I.

TABLE I. IEEE 9-Bus Network Inertia Configuration

Case	G1 Machine (247 MVA)	G2 Machine (192 MVA)	G3 Machine (128 MVA)	Total Inertia (MVA.s)
Base	H = 9.55 2364 MVA.s	H = 3.92 753 MVA.s	H = 2.77 355 MVA.s	3470
80% G1	H = 11.2 2771 MVA.s	H = 2.3 442 MVA.s	H = 2.0 256 MVA.s	3470
90% G1	H = 12.6 3118 MVA.s	H = 1.1 211 MVA.s	H = 1.1 141 MVA.s	3470
95% G1	H = 13.3 3291 MVA.s	H = 0.6 115 MVA.s	H = 0.5 64 MVA.s	3470

C. Results

For each of the cases listed in Table I, a time-based RMS simulation was carried out and the system frequency and RoCoF was calculated at Bus 1, Bus 2, and Bus 3, based on the machine frequency in order to obtain the most accurate results. The system frequency as measured by the machine speed can be seen in Fig. 4, where it is observed that the frequency deviation of the G1 machine remains similar in all cases, but the frequency deviation in the G2 and G3 machines

This article has been accepted for publication in a future proceedings of this conference, but has not been fully edited. Content may change prior to final publication. Citation information: DOI10.1109/UPEC57427.2023.10295005, 2023 58th International Universities Power Engineering Conference (UPEC)

becomes more pronounced as the system inertia centre becomes more concentrated at the G1 machine.

The COI frequency is also recorded and can be seen converging in value to the G1 machine frequency, as the inertia becomes more concentrated at the G1 machine. The system frequency was also measured with an untuned PLL, set as per Part III, section C, and the results can be seen in Fig. 5, which show some significant variations in response shapes and magnitudes.

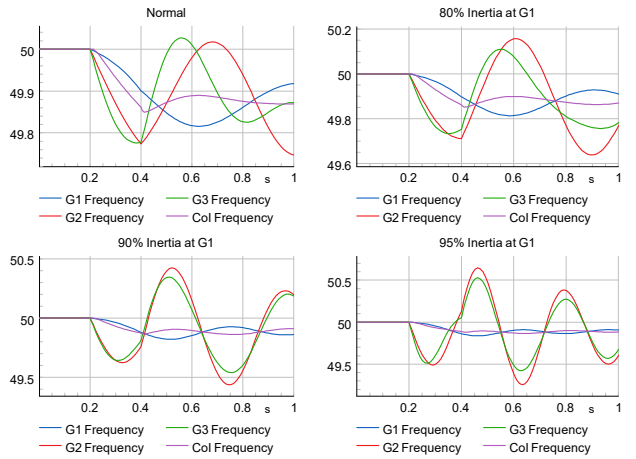

Fig. 4. IEEE 9-Bus Model Frequency Results (Machine Measurement)

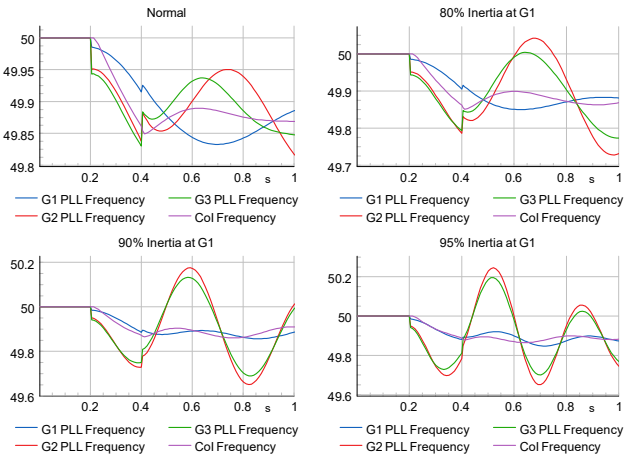

Fig. 5. IEEE 9-Bus Model Frequency Results (Untuned PLL Measurement)

For reference purposes the machines RoCoF was also recorded based on a 500 ms moving average window, based on the NG ESO / ENTSO-E guidelines noted in Section I-E, for each of the cases, as RoCoF is critical parameter for determination of potential problems for LoM protection operating. The results can be seen in Fig. 6, where in the 90% inertia case RoCoF becomes marginal for the G2 machine, and in the 95% inertia case, the RoCoF exceeds the typical 1 Hz/s limit of most TSOs.

D. Inertia Distribution Index Calculation

As noted in Part II, section B, the use of an IDI based approach has been adopted by researchers to help identify the weak / low inertia nodes in the system. The results for the IDI calculation for each of the inertia loading cases can be seen in Table II for both the direct measurement approach and the use of the untuned PLL. From this table a potential weakness is identified with the IDI approach, as whilst it indicates that a node may be more vulnerable to localized frequency disturbances it does not indicate which locations are likely to exceed a specific RoCoF limit.

Looking at the results of the 90% and 95% case in Fig. 5, G2 and G3 have similar results, but the calculated IDI values are very different, and it would be easy to overlook the vulnerability of the G3 machine, if only an IDI value-based approach is used. When the results of the IDI process are compared it is noted that there can be some significant variance between the Direct Measurement and the untuned PLL measurement, which can add further uncertainty to the results.

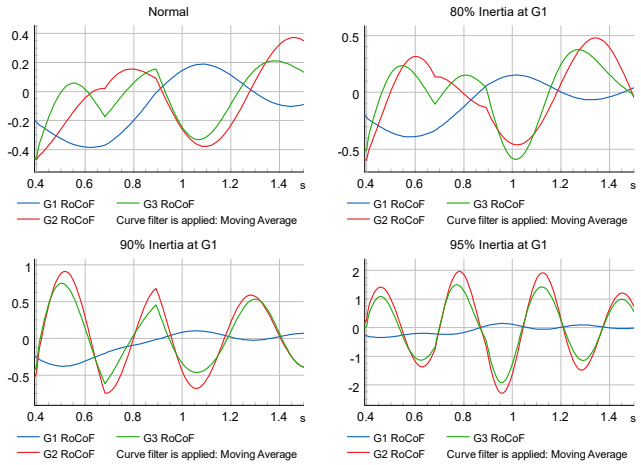

Fig. 6. IEEE 9-Bus Model RoCoF Results

TABLE II. IEEE 9-BUS NETWORK IDI RESULTS

Case	G1 Machine IDI		G2 Machine IDI		G3 Machine IDI	
	Direct	PLL	Direct	PLL	Direct	PLL
Base	0.27	0.83	1.0	1.0	0.78	0.46
80% G1	0.1	0.11	1.0	1.0	0.57	0.58
90% G1	0.02	0.02	1.0	1.0	0.74	0.75
95% G1	0.01	0.01	1.0	1.0	0.65	0.73

It has been shown that the use of an IDI based approach to distributed inertia must be used with care, and potentially faces several practical difficulties. Systems with heavily centralized inertia can produce IDI values that might appear as satisfactory but are vulnerable to high levels of localized frequency variation. It was also shown that the use of frequency measurement technique must also be considered as the use of simple bus estimates of frequency or a poorly tuned PLL can give misleading values.

E. Alternative Comparison

A simpler method can be adopted, where the local machine frequency is compared to the COI frequency, as a continuous function, and the difference used to identify weak nodes. This approach is mathematically simpler than the square integral form and returns a result directly in Hz.

Using an alternative method of a simple difference calculation, the weakness of a remote machine / busbar can be simply calculated with the analysis software, and then categorized, based on a simple magnitude value such as ±0.25 Hz, or ±0.5 Hz. This method allows a more rapid identification

This article has been accepted for publication in a future proceedings of this conference, but has not been fully edited. Content may change prior to final publication. Citation information: DOI10.1109/UPEC57427.2023.10295005, 2023 58th International Universities Power Engineering Conference (UPEC)

of nodes and the magnitude of the any potential areas where the frequency difference becomes large. Results for this approach can be seen in Fig. 8 and Table III.

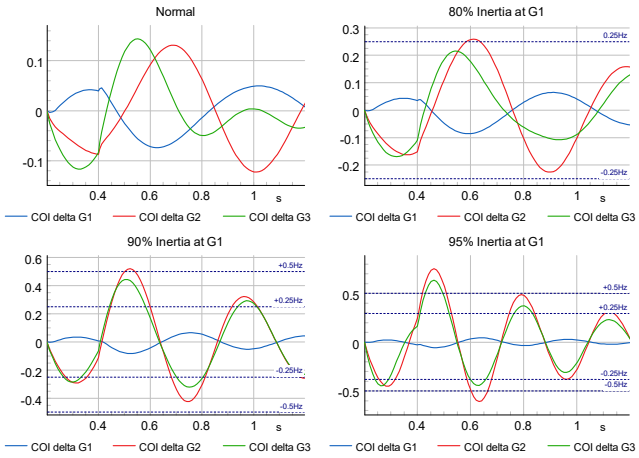

Fig. 7. IEEE 9-Bus Model Frequency Difference Results

TABLE III. IEEE 9-BUS NETWORK IDI RESULTS

Case	G1 Machine Δf_{max} (Hz)	G2 Machine Δf_{max} (Hz)	G3 Machine Δf_{max} (Hz)
Base	0.05	0.131	0.144
80% G1	0.065	0.26	0.21
90% G1	0.065	0.52	0.44
95% G1	0.04	0.75	0.63

V. CONCLUSIONS & FURTHER WORK

The analysis within the paper indicated that inertia distribution is a topic of significant interest for embedded generation as the inertia distribution creates significant localized variations in the system frequency and RoCoF behaviour. It was identified that the method of frequency measurement used on typical RMS simulation packages can often lead to some significant errors in values, as different approaches and calculation methods are used, that may not be immediately obvious. It was further identified that the currently used integral square difference approach to calculate an IDI of an uneven inertia distribution, can provide misleading results in systems with a very uneven distribution of inertia, and a simpler difference calculation with the COI frequency gives more readily accessible results, that are tolerant of localized significant variations.

Further work in this area would be to expand the analysis to larger test networks to see if further breakdown of the IDI approach also occurs, and if the suggested frequency difference method is sufficiently robust. An alternative approach for calculating inertia distribution impacts is currently under investigation based on the comparison of RoCoF between localized busbars and the COI RoCoF.

REFERENCES

[1] Kundur P., *Power System Stability and Control*. McGraw Hill, 1994.

[2] IEEE, "PES TR-77: Definition and Classification of Power System Stability Revisited," 2020.

[3] P. Tielens and D. Van Hertem, "The relevance of inertia in power systems," *Renewable and Sustainable Energy Reviews*, vol. 55, pp. 999–1009, Mar. 2016, doi: 10.1016/j.rser.2015.11.016.

[4] M. Trujillo, R. W. Kenyon, G. Yau, L. Yu, A. Hoke, and B.-M. Hodge, "Operability of a Power System with Synchronous Condensers and Grid-Following Inverters," in *2022 IEEE 49th Photovoltaics Specialists Conference (PVSC)*, IEEE, Jun. 2022, pp. 1038–1042. doi: 10.1109/PVSC48317.2022.9938954.

[5] J. Dhanuja Lekshmi, Z. H. Rather, and B. C. Pal, "Frequency Response Improvement in RE Integrated Low Inertia Power Systems using Synchronous Condensers," in *2022 22nd National Power Systems Conference (NPSC)*, IEEE, Dec. 2022, pp. 602–607. doi: 10.1109/NPSC57038.2022.10069861.

[6] Md. N. Haque Shazon, H. M. Ahmed, Nahid-Al-Masood, and F. Hasan, "Supplementary Inertial Support in Renewable Integrated Networks: Potential of Synchronous Condenser and Energy Storage," in *2021 IEEE PES Innovative Smart Grid Technologies Europe (ISGT Europe)*, IEEE, Oct. 2021, pp. 1–5. doi: 10.1109/ISGTEurope52324.2021.9640010.

[7] V. Arayamparambil Vinaya Mohanan, I. M. Y. Mareels, R. J. Evans, and R. R. Kolluri, "Stabilising influence of a synchronous condenser in low inertia networks," *IET Generation, Transmission & Distribution*, vol. 14, no. 17, pp. 3582–3593, Sep. 2020, doi: 10.1049/iet-gtd.2020.0178.

[8] M. Nedd, C. Booth, and K. Bell, "Potential solutions to the challenges of low inertia power systems with a case study concerning synchronous condensers," in *2017 52nd International Universities Power Engineering Conference (UPEC)*, IEEE, Aug. 2017, pp. 1–6. doi: 10.1109/UPEC.2017.8232001.

[9] A. Adrees, J. V. Milanović, and P. Mancarella, "Effect of inertia heterogeneity on frequency dynamics of low-inertia power systems," *IET Generation, Transmission & Distribution*, vol. 13, no. 14, pp. 2951–2958, Jul. 2019, doi: 10.1049/iet-gtd.2018.6814.

[10] T. Xu, W. Jang, and T. J. Overbye, "Investigation of inertia's locational impacts on primary frequency response using large-scale synthetic network models," in *2017 IEEE Power and Energy Conference at Illinois (PECI)*, IEEE, Feb. 2017, pp. 1–7. doi: 10.1109/PECI.2017.7935742.

[11] B. A. Osbouei, G. A. Taylor, O. Bronckart, J. Maricq, and M. Bradley, "Impact of Inertia Distribution on Power System Stability and Operation," in *2019 IEEE Milan PowerTech*, IEEE, Jun. 2019, pp. 1–6. doi: 10.1109/PTC.2019.8810689.

[12] T. Xu, Y. Liu, and T. J. Overbye, "Metric development for evaluating inertia's locational impacts on system primary frequency response," in *2018 IEEE Texas Power and Energy Conference (TPEC)*, IEEE, Feb. 2018, pp. 1–6. doi: 10.1109/TPEC.2018.8312056.

[13] D. Doheny and M. Conlon, "Investigation into the local nature of rate of change of frequency in electrical power systems," in *2017 52nd International Universities Power Engineering Conference (UPEC)*, IEEE, Aug. 2017, pp. 1–6. doi: 10.1109/UPEC.2017.8231982.

[14] S. Azizi, M. Sun, G. Liu, and V. Terzija, "Local Frequency-Based Estimation of the Rate of Change of Frequency of the Center of Inertia," *IEEE Transactions on Power Systems*, vol. 35, no. 6, pp. 4948–4951, Nov. 2020, doi: 10.1109/TPWRS.2020.3014818.

[15] Y. Wang, H. Silva-Saravia, and H. Pulgar-Painemal, "Estimating inertia distribution to enhance power system dynamics," in *2017 North American Power Symposium (NAPS)*, IEEE, Sep. 2017, pp. 1–6. doi: 10.1109/NAPS.2017.8107383.

[16] National Grid ESO, "Security & Quality of Supply Standards Frequency Risk and Control Policy," 2020.

[17] ENTSO-E, "System Needs Study System dynamic and operational challenges," 2022.

[18] ENTSO-E, "Rate of Change of Frequency (RoCoF) withstand capability," 2018.

[19] AEMO, "Advice Reliability Panel Review of Frequency Operating Standard," 2022.

[20] CIGRE, "CIGRE TB 881 - CIGRE TB 881 Electromagnetic transient simulation models for large-scale system impact studies in power systems having a high penetration of inverter-connected generation," 2022.